ISSN 0554-6397
UDK: 621.43.016
629.5.03-81
Preliminary communication
Received: 30.01.2019.

Vedran Mrzljak
Email: vedran.mrzljak@riteh.hr
Faculty of Engineering, University of Rijeka, Vukovarska 58, 51000 Rijeka, Croatia
Nikola Anđelić
Email: nandelic@riteh.hr
Faculty of Engineering, University of Rijeka, Vukovarska 58, 51000 Rijeka, Croatia
Igor Poljak
Email: ipoljak1@unizd.hr
Department of Maritime Sciences, University of Zadar, Mihovila Pavlinovića 1, 23000 Zadar, Croatia
Josip Orović
Email: jorovic@unizd.hr
Department of Maritime Sciences, University of Zadar, Mihovila Pavlinovića 1, 23000 Zadar, Croatia

Thermodynamic analysis of marine steam power plant pressure reduction valves

Abstract

The paper presents a thermodynamic analysis of pressure reduction valves from a marine steam power plant that operates on conventional LNG carriers. The analysis refers to six condensate and superheated steam pressure reduction valves. Based on the exploitation data, the calculation involves the energy/exergy flow streams as well as the exergy efficiency and exergy destruction of each pressure reduction valve. The analysis also included the influence of changes in the ambient temperature on the efficiency and destruction of each valve. Total energy and exergy fluid flow streams through each valve showed the same trends. The superheated steam pressure reduction valves showed a lower average exergy destruction rate and higher average exergy efficiency compared with the water/condensate ones. Increase in the ambient temperature resulted in a continuous increase in the exergy destruction rate and a continuous decrease in exergy efficiency in all the observed pressure reduction valves. Pressure reduction valves of high exergy destruction rate and low exergy efficiency are notably influenced by changes in the ambient temperature.

Keywords: pressure reduction, valve, marine steam plant, thermodynamic analysis, ambient temperature

1. Introduction

Marine propulsion plants on commercial ships are nowadays mainly based on diesel engines. In general, the most used ship propulsion engines are slow-speed two-stroke diesel engines [1, 2], while the medium-speed and fast-speed four-stroke diesel engines can be found in engine rooms of many ships in different combinations and with various functions (the most usual function of such diesel engines is the electric generator drive) [3, 4].

Marine propulsion with steam power plant is still today the dominant propulsion of LNG (Liquefied Natural Gas) carriers [5] due to the specificity of transported cargo. The question for the near future is whether this fact will be still valid because the impact of diesel engines has been increasing on a daily basis in engine rooms of LNG carriers [6] as well, especially after the development of dual fuel diesel engines using both diesel fuel and natural gas [7, 8].

Scientific and professional literature offers an energy efficiency analysis of various LNG carrier powering options [9] as well as several proposals of new propulsion power plants [10] that offer many improvements (compared with the currently used ones). An LNG carrier propulsion power plant is not the only component that can be improved because the improvement of cargo transport, manipulation and heat loss minimization can also bring many benefits [11]. During the LNG carrier operation, the produced waste heat can be used in additional systems aimed at reducing greenhouse gas emissions [12] or in ORC (Organic Rankine Cycle) systems aimed at producing additional power [13].

Marine power plants on LNG carriers along with their additional components can be regarded as complex systems requiring proper computer software for power management [14] and maintenance [15] as well as multi-objective decision support systems [16].

This paper deals with an analysis of pressure reduction valves that operate on more recent LNG carrier steam power plant that includes steam re-heating. Power plant consists of six pressure reduction valves - three of them to reduce the superheated steam pressure and the other three to reduce the water/condensate pressure. Without proper operation of analyzed pressure reduction valves, steam power plant running would be very difficult or even impossible. The energy/exergy flow streams were calculated in respect of each valve, in addition to the operating fluid pressure and temperature reductions as well as the exergy efficiency and exergy destruction rates. A detailed explanation of efficiencies and losses of pressure reduction valves could only be obtained from the exergy aspect. At the end, the influence of changes in the ambient temperature on the operation of each pressure reduction valve was analyzed.

2. Marine steam power plant description with characteristics of pressure reduction valves and their influence on plant operation

This analysis dealt with the selected marine steam power plant that is used for the propulsion of conventional LNG carriers [17]. The selected steam power plant is provided with additional steam re-heating that improves plant operation and increases its overall efficiency. This power plant is a newer version of marine steam power plant older versions that are not provided with additional steam re-heating.

Figure 1 presents a general scheme of the selected steam power plant provided with steam re-heating.

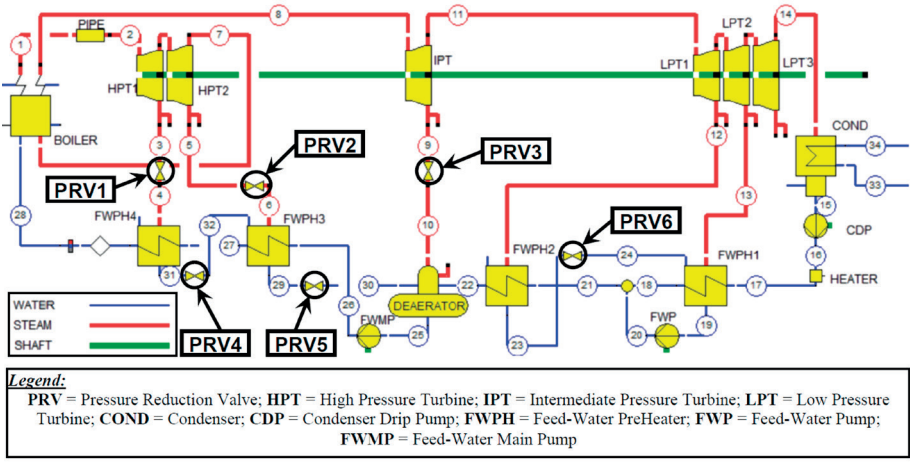

Figure 1 – General scheme of the LNG carrier steam power plant with marked pressure reduction valves used for the thermodynamic analysis [17]

The marine steam power plant selected for the pressure reduction valves thermodynamic analysis to be dealt with in this paper consists of a steam generator (boiler) with additional steam re-heating, Figure 1. Usually, a marine steam power plant has two parallel operating steam generators [18] to ensure continuous superheated steam supply. Figure 1 presents only the main steam stream, without the auxiliary steam stream (steam with decreased temperature compared with the main steam stream). The auxiliary steam stream is used in marine steam plant for additional heating purposes (for example, in the steam generator air heater [19] and in some operating regimes for de-aerator and feed-water pre-heater additional heating) as well as in auxiliary ship systems [20]. In marine steam power plant, flue gases from steam generator(s) usually do not reach sufficient temperature for air heating (air heating must be performed with the auxiliary steam stream), what represents a completely

different operation logic compared with air heaters operating in land-based steam power plants [21, 22] where flue gases have sufficient temperature for air heating.

While heat losses occur in all steam and water pipelines, the most intensive heat loss occurs in the pipeline between the steam generator(s) and the main propulsion turbine (points from 1 to 2, Figure 1) due to the highest steam pressure and temperature. Marine steam power plant with steam re-heating consists of three main propulsion turbine cylinders (high pressure, intermediate pressure and low pressure), as presented in Figure 1. In marine steam propulsion plants without steam re-heating, the main propulsion turbine is provided with only two cylinders (high pressure and low pressure), [23, 24]. Steam was extracted from all the main propulsion turbine cylinders, to be used for heating in feed-water pre-heaters.

The main steam stream in the marine propulsion power plant was led not only to the main propulsion turbine but also to turbo-generators [25] for the production of electricity and to the low power steam turbine [26] for the main feed-water pump drive (turbo-generators and low power steam turbine for the main feed-water pump drive are additional turbines which are not presented in the general scheme of marine steam power plant in Figure 1). After having passed all the turbines the steam stream was led to the main condenser where its condensation took place. The marine main steam condenser operation can differ greatly when compared to main steam condensers from land-based power plants [27, 28].

After steam condensation in the main condenser, the obtained condensate pressure is increased by the condenser drip pump (CDP) [29] and the condensate is delivered from the main steam condenser to the de-aerator. Between the main steam condenser and de-aerator the condensate/feed-water passes through several low pressure pre-heaters that increase the condensate/feed-water temperature. The first of such low pressure pre-heaters seals the steam condenser (gland steam condenser denominated just as a heater in Figure 1) [30]. With the steam condenser sealing completed, the observed marine steam power plant has two low pressure feed-water pre-heaters [31].

De-aerator in marine steam power plant, as well as in the land-based steam power plant, has two functions – the first is heating of the condensate/feed-water [32] and the second one is dissolving gas removal from the condensate/feed-water [33]. Between the de-aerator and steam generator (boiler) in the observed marine steam power plant there are mounted two high pressure feed-water pre-heaters [34] that are used for additional feed-water temperature increase [35]. The entire condensate/feed-water heating system in any steam power plant (marine and land-based) is used for increasing the condensate/feed-water temperature before it reaches the steam generator, thus reducing fuel consumption and increasing the steam system overall efficiency [36, 37].

Pressure reduction valves (PRV) in the marine steam power plant, Figure 1, is used for decreasing the operating fluid (superheated steam and condensate) pressure. Simultaneously with a decrease in pressure, pressure reduction valves decreases the

operating fluid temperature [38]. As the authors in [17] declare, pressure reduction valves are used to validate the marine steam power plant simulation (in order for the simulation to give the power plant operating parameters similar to the measurements, as close as possible). Decreasing of the operating fluid pressure is very important in marine steam power plants as in such a way the weight of power plant components can be held within reasonable limits, while each component simultaneously fulfills its main function. Therefore, pressure reduction valves are much more used in marine steam power plants compared with land-based steam power plants.

Steam power plant presented in Figure 1 has six pressure reduction valves. Three of them (PRV1, PRV2 and PRV3) reduce the superheated steam pressure, while the other three are used for reducing the condensate pressure (PRV4, PRV5 and PRV6). PRV1 and PRV2 are used for reducing pressure of the superheated steam extracted from the high pressure steam turbine and led to high pressure feed-water pre-heaters (FWPH3 and FWPH4). PRV3 also reduces the superheated steam pressure, which is extracted from the intermediate pressure turbine and led to the de-aerator. The PRV4 reduces pressure of the condensate that is led from the second (FWPH4) to the first (FWPH3) feed-water high pressure pre-heater. The PRV5 reduces pressure of the condensate that is led from the first high pressure feed-water pre-heater (FWPH3) to de-aerator, while the PRV6 reduces pressure of the condensate that is led from the second low pressure feed-water pre-heater (FWPH2) to the first low pressure feed-water pre-heater (FWPH1).

Operating parameters of a marine steam power plant at full load (pressures, temperatures and mass flow rates of each operating fluid stream) are presented in [17], yet a detailed analysis of pressure reduction valves was not performed. Therefore, this paper deals not only with the performance of the thermodynamic analysis of the presented pressure reduction valves (analysis of each pressure reduction valve loss and efficiency) but also with the investigation of the influence of the ambient temperature change on the operation of each pressure reduction valve.

3. Equations for the pressure reduction valve thermodynamic analysis

3.1. Thermodynamic analysis of a control volume – overall equations

Thermodynamic analysis of any control volume (as well as of each observed pressure reduction valve analyzed in this paper) includes a calculation of control volume losses and efficiencies. Thermodynamic analysis can be performed in two different ways – from the aspect of energy and exergy. Energy analysis is based on the first law of thermodynamics [39] and it does not include the parameters of the ambient (ambient pressure and temperature) in which the control volume operates [40]. Exergy analysis is based on the second law of thermodynamics [41] and it includes the parameters of the ambient in which the control volume operates [11].

3.1.1. Energy analysis of a control volume

When disregarding the potential and kinetic energy, for any control volume in steady state the mass flow rate and energy balances are defined according to [42] and [43] as:

$$\sum \dot{m}_{\text{in}} = \sum \dot{m}_{\text{out}}, \tag{1}$$

$$\sum \dot{m}_{\text{in}} \cdot h_{\text{in}} + \dot{Q} = \sum \dot{m}_{\text{out}} \cdot h_{\text{out}} + P. \tag{2}$$

The total energy of a flow according to [44] is:

$$\dot{E}_{\text{en}} = \dot{m} \cdot h. \tag{3}$$

The energy efficiency of a control volume is defined by its operating characteristics. Therefore, energy efficiency of a control volume can have different forms [45, 46]. In most cases the general definition of the control volume energy efficiency is:

$$\eta_{\text{en}} = \frac{\text{Energy output}}{\text{Energy input}}. \tag{4}$$

3.1.2. Exergy analysis of a control volume

The exergy balance equation for a control volume in steady state, disregarding the potential and kinetic energy, can be defined according to [47] and [48] as:

$$\sum \dot{m}_{\text{in}} \cdot \varepsilon_{\text{in}} + \dot{X}_{\text{heat}} = \sum \dot{m}_{\text{out}} \cdot \varepsilon_{\text{out}} + P + \dot{E}_{\text{ex,D}}. \tag{5}$$

Specific exergy according to [49] and [50] is defined as:

$$\varepsilon = (h - h_0) - T_0 \cdot (s - s_0). \tag{6}$$

The net exergy transfer by heat ($\dot{X}_{\text{heat}}$) at the temperature T, according to [51] and [52] is defined as:

$$\dot{X}_{\text{heat}} = \sum (1 - \frac{T_0}{T}) \cdot \dot{Q}. \tag{7}$$

The total exergy of a flow according to [53] is defined by an equation:

$$\dot{E}_{\text{ex}} = \dot{m} \cdot \varepsilon = \dot{m} \cdot \left[(h - h_0) - T_0 \cdot (s - s_0) \right]. \tag{8}$$

The second law efficiency or effectiveness is another term for the control volume exergy efficiency [54]. Similar to energy efficiency, characteristics of the control

volume operation define its exergy efficiency. The general definition of the control volume exergy efficiency according to [55] and [56] is:

$$\eta_{ex} = \frac{\text{Exergy output}}{\text{Exergy input}}. \tag{9}$$

3.2. Thermodynamic analysis of the pressure reduction valve

Thermodynamic analysis of any pressure reduction valve can be performed with the same equations [38]. In this paper equations will be presented for thermodynamic analysis of PRV1 (Figure 1). Thermodynamic analysis of pressure reduction valve is based on operating fluid parameters (temperature, pressure and mass flow rate) at valve inlet and outlet. As declared in Figure 1, operating parameters of superheated steam at PRV1 inlet are marked with number 3, while operating parameters of superheated steam at PRV1 outlet are marked with number 4.

3.2.1. Energy analysis of pressure reduction valve

Pressure reduction valves are steam power plant components whose energy analysis, during the usual operation, will result in the energy power loss (energy destruction) equal to zero and simultaneously in energy efficiency equal to 100%. Along with pressure reduction valves (throttle valves) [39], there is another steam power plant component whose energy analysis will give the same result (during the usual operation), i.e.a steam turbine labyrinth seal [57]. Therefore, the only relevant thermodynamic analysis of pressure reduction valve (or labyrinth seal) is exergy analysis. This conclusion will be explained in detail farther in this section.

- The energy power input of PRV1 is:

$$\dot{E}_{en,in,PRV1} = \dot{m}_{in,PRV1} \cdot h_{in,PRV1} = \dot{m}_3 \cdot h_3. \tag{10}$$

- The energy power output of the same PRV1 is:

$$\dot{E}_{en,out,PRV1} = \dot{m}_{out,PRV1} \cdot h_{out,PRV1} = \dot{m}_4 \cdot h_4. \tag{11}$$

- Energy power loss (energy destruction) of PRV1 is defined as:

$$\dot{E}_{en,D,PRV1} = \dot{E}_{en,in,PRV1} - \dot{E}_{en,out,PRV1} = \dot{m}_3 \cdot h_3 - \dot{m}_4 \cdot h_4. \tag{12}$$

- Energy efficiency of PRV1 is:

$$\eta_{en,PRV1} = \frac{\dot{E}_{en,out,PRV1}}{\dot{E}_{en,in,PRV1}} = \frac{\dot{m}_4 \cdot h_4}{\dot{m}_3 \cdot h_3}. \tag{13}$$

During the usual operation of any pressure reduction valve, the leakage of operating fluid mass flow rate does not occur. Therefore, the equation of mass flow rates at PRV1 input (inlet) and output (outlet) is:

$$\dot{m}_{\text{in,PRV1}} = \dot{m}_{\text{out,PRV1}} \quad \rightarrow \quad \dot{m}_3 = \dot{m}_4 \,. \tag{14}$$

Pressure reduction valve reduces the operating fluid pressure (and simultaneously the operating fluid temperature), but the operating fluid specific enthalpy (heat content) throughout the pressure reduction valve remains constant during the usual operation [58, 59]. The only decrease in the operating fluid specific enthalpy can occur during heat losses on the valve, but such decrease in specific enthalpy is small and in most cases neglectable [38]. So, for the superheated steam specific enthalpy at PRV1 input (inlet) and output (outlet) the following equation is valid:

$$h_{\text{in,PRV1}} = h_{\text{out,PRV1}} \quad \rightarrow \quad h_3 = h_4 \,. \tag{15}$$

The same mass flow rates at the PRV1 inlet and outlet, Eq. (14) and the same specific enthalpies at the PRV1 inlet and outlet, Eq. (15) resulted in the fact that the energy power input and output, Eq. (10) and Eq. (11) of observed PRV1 are equal. Equal energy power input and output resulted in the PRV1 energy destruction equal to zero, Eq. (12) and in PRV1 energy efficiency equal to 100%, Eq. (13). This observation is valid for any pressure reduction valve during the usual operation (with no mass flow leakage and with no intense heat losses).

The total energy of a fluid flow throughout any pressure reduction valve, according to conclusions above, is:

$$\dot{E}_{\text{en,TOT}} = \dot{E}_{\text{en,in}} = \dot{E}_{\text{en,out}} = \dot{m}_{\text{in}} \cdot h_{\text{in}} = \dot{m}_{\text{out}} \cdot h_{\text{out}} \,. \tag{16}$$

3.2.2. Exergy analysis of pressure reduction valve

Each pressure reduction valve, as stated earlier, reduces the operating fluid pressure and temperature while the operating fluid specific enthalpy remains constant. Such operation also resulted in an increase in the operating fluid specific entropy, meaning that the operating fluid specific exergy, Eq. (6), will not be the same at the pressure reduction valve input (inlet) and output (outlet). Therefore, it is only the exergy analysis of any pressure reduction valve to be considered relevant for observing valve loss and efficiency.

For the PRV1, equations for the exergy analysis are:

- Exergy power input of PRV1:

$$\dot{E}_{\text{ex,in,PRV1}} = \dot{m}_{\text{in,PRV1}} \cdot \varepsilon_{\text{in,PRV1}} = \dot{m}_3 \cdot \varepsilon_3 \,. \tag{17}$$

- Exergy power output of PRV1:

$$\dot{E}_{\text{ex,out,PRV1}} = \dot{m}_{\text{out,PRV1}} \cdot \varepsilon_{\text{out,PRV1}} = \dot{m}_4 \cdot \varepsilon_4 . \tag{18}$$

- Exergy power loss (exergy destruction) of PRV1:

$$\dot{E}_{\text{ex,D,PRV1}} = \dot{E}_{\text{ex,in,PRV1}} - \dot{E}_{\text{ex,out,PRV1}} = \dot{m}_3 \cdot \varepsilon_3 - \dot{m}_4 \cdot \varepsilon_4 . \tag{19}$$

- Exergy efficiency of PRV1:

$$\eta_{\text{ex,PRV1}} = \frac{\dot{E}_{\text{ex,out,PRV1}}}{\dot{E}_{\text{ex,in,PRV1}}} = \frac{\dot{m}_4 \cdot \varepsilon_4}{\dot{m}_3 \cdot \varepsilon_3} . \tag{20}$$

The same exergy analysis equations from (17) to (20) are also used for the exergy analysis of any other observed pressure reduction valve from the marine steam power plant, according to operating fluid stream flow marks in Figure 1.

4. Fluid operating parameters at analyzed pressure reduction valves inlet and outlet

Operating fluid parameters of each observed pressure reduction valve (pressure, temperature and mass flow rate) at valve inlet and outlet are found in [17] and presented in Table 1, according to Figure 1. Condensate/steam specific enthalpies and specific entropies are calculated from known pressure and temperature values at each valve inlet and outlet by using NIST-REFPROP 9.0 software [60].

Table 1 also presents specific exergies of each fluid stream at each valve inlet and outlet, calculated according to Eq. (6). Specific exergy of each fluid stream is dependable on conditions of the analyzed pressure reduction valves operation ambient. Base ambient conditions in this analysis are:

- pressure: $p_0 = 100$ kPa = 1 bar,
- temperature: $T_0 = 288$ K = 15 °C.

Base ambient conditions are used in the first part of the analysis. In the second part of the analysis, ambient pressure remains the same as in base ambient conditions while the ambient temperature is varied from 278 K to 313 K. Variation of the ambient temperature is performed in the real temperature range that can be expected at an LNG carrier steam power plant during exploitation. The ambient pressure change during the real power plant operating conditions is small and its change can be neglected.

Energy analysis of each component of the marine steam power plant (or any other power plant) is not influenced by the ambient temperature change. On the other hand, the ambient temperature change has influenced the specific exergy of each fluid stream, Eq. (6) – therefore, the exergy analysis of any power plant component is

influenced by the ambient temperature change. The proper question in respect of the analyzed pressure reduction valves is whether the change in the ambient temperature has influenced each valve equally? The answer to this question is presented in the second part of the performed analysis.

Table 1 – Operating fluid parameters at each observed pressure reduction valve inlet and outlet

Pressure reduction valve (according to Figure 1)	Operating point* (according to Figure 1)	Mass flow rate (kg/s)	Temperature (K)	Pressure (kPa)	Specific enthalpy (kJ/kg)	Specific entropy (kJ/kg·K)	Specific exergy (kJ/kg)
PRV1	**3**	1.055	671.01	3870	3211.70	6.782	1260.10
	4	1.055	670.26	3770	3211.70	6.793	1256.90
PRV2	**5**	1.679	599.95	2260	3079.20	6.809	1119.90
	6	1.679	598.44	2120	3079.20	6.837	1111.80
PRV3	**9**	0.421	614.95	560	3149.80	7.553	976.05
	10	0.421	614.54	520	3149.80	7.587	966.28
PRV4	**31**	1.055	519.87	3770	1069.90	2.764	275.53
	32	1.055	488.49	2120	1069.90	2.777	271.70
PRV5	**29**	2.734	488.35	2120	921.45	2.473	210.77
	30	2.734	426.46	520	921.45	2.520	197.22
PRV6	**23**	0.808	399.07	240	528.99	1.591	72.24
	24	0.808	359.08	60	528.99	1.616	65.05

** For each pressure reduction valve the first row is valve input (inlet) and the second one is valve output (outlet)*

5. Results of the pressure reduction valves thermodynamic analysis with discussion

5.1. Thermodynamic analysis of pressure reduction valves at base ambient conditions

The total energy of any fluid flow stream is defined by Eq. (3) as a product of the fluid mass flow rate and its specific enthalpy (specific enthalpy can be obtained from fluid current pressure and temperature). According to conclusions of the pressure reduction valve energy analysis, the total energy of fluid flow is the same at each pressure reduction valve inlet and outlet.

As presented in Figure 2, the highest energy of fluid flow refers to PRV2 (5169.98 kW) followed by PRV1 (3388.34 kW) - two pressure reduction valves that operate with superheated steam of the highest temperature (compared with temperatures of fluid streams passing through other pressure reduction valves). The lowest energy of fluid flow refers to PRV6 (427.42 kW). The condensate passing through PRV6 has the lowest pressure and temperature compared with other observed fluid streams, Table 1.

On the average, the total fluid flow energy is much higher for pressure reduction valves operating with superheated steam (PRV1, 2 and 3) compared with those operating with condensate (PRV4, 5 and 6). The same trend as obtained for the total energy of each fluid flow will be also valid for total exergy of each fluid flow.

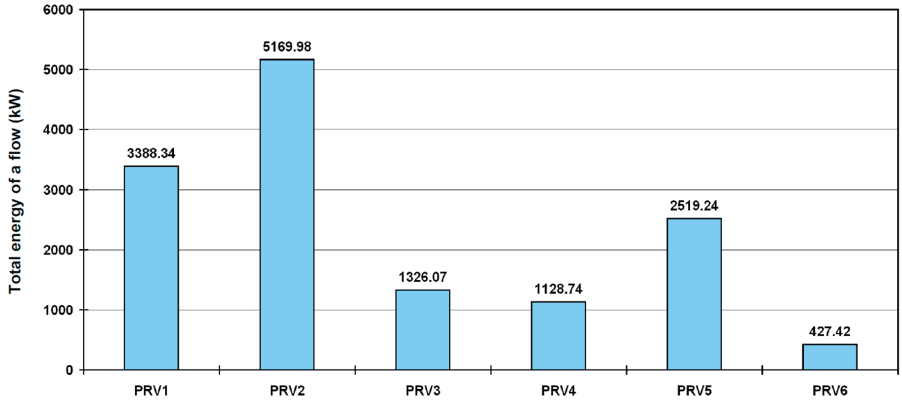

Figure 2 – Total energy of a flow through each observed pressure reduction valve

Each observed pressure reduction valve, as stated before, decreases the operating fluid pressure and simultaneously decreases the operating fluid temperature while the specific enthalpy remains the same before and after the valve. As presented in Figure 3, reduction in the operating fluid pressure and temperature is low if the superheated steam operates the fluid that passes through a valve (PRV1, 2 and 3).

Pressure reduction valves operating with condensate cause significant decreases in the condensate pressure and temperature (PRV 4, 5 and 6). The highest decrease in condensate pressure can be observed at PRV4 (1650 kPa) and at PRV5 (1600 kPa), while the highest decrease in condensate temperature is observed at PRV5 (61.89 K), Figure 3.

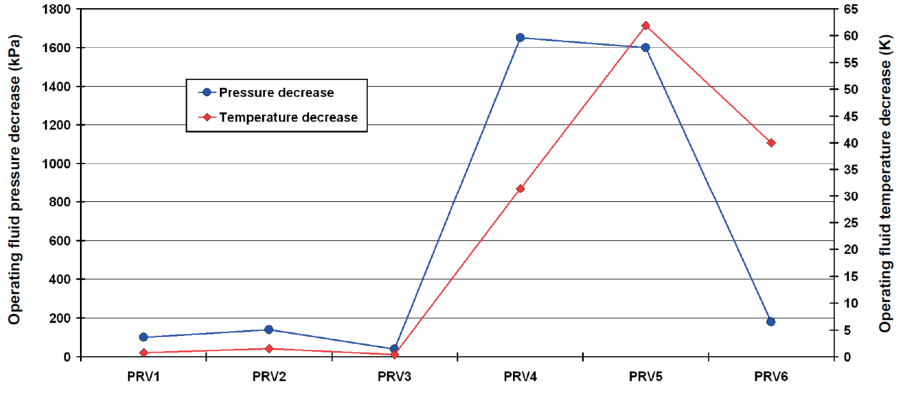

Figure 3 – Decrease in operating fluid pressure and temperature while passing through a pressure reduction valve

The trend of the total energy of each fluid flow, Figure 2, is the same as the trend of the total exergy of each fluid flow, Figure 4. The total flow exergy highest values can be observed for PRV1 and PRV2, while the lowest total flow exergy refers to PRV6. Similar to the total energy of any fluid flow, the average value of total flow exergy is notably higher for pressure reduction valves that operate with superheated steam compared with valves that operate with condensate.

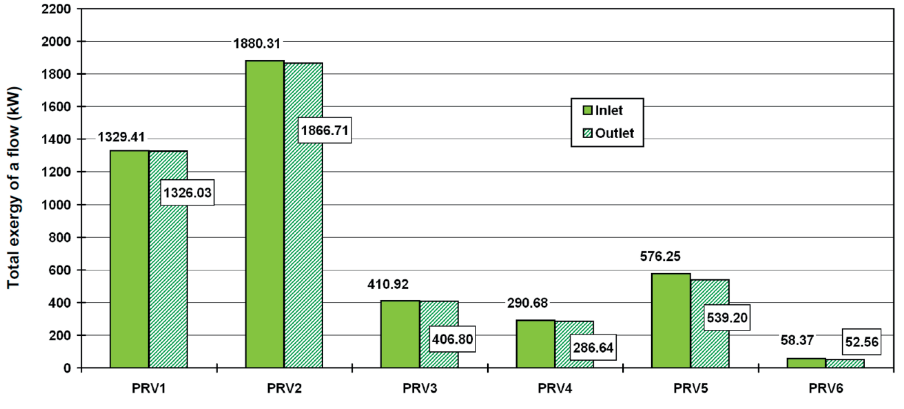

Figure 4 – Total exergy of a flow at each pressure reduction valve inlet and outlet

The total exergy of any fluid flow (superheated steam or condensate) is calculated for each pressure reduction valve inlet and outlet by using Eq. 8. Due to changes in the operating fluid specific entropy while passing through the valve, a change also occurs in the fluid specific exergy and therefore the total exergy of fluid flow is not the same before and after each pressure reduction valve. Differences between the total fluid exergy at the pressure reduction valve inlet and outlet define the exergy efficiency and exergy destruction (exergy loss) of each valve.

Exergy destruction of each pressure reduction valve is the difference between the total exergy of fluid flow at the valve inlet and the total exergy of fluid flow at the valve outlet. Figure 5 shows that the highest exergy destruction for pressure reduction valves that operate with superheated steam is calculated for PRV2 (13.60 kW), while in respect of the valves that operate with condensate the highest exergy destruction is calculated for PRV5 (37.05 kW). Pressure reduction valves that operate with superheated steam show a lower average exergy destruction compared with those that operate with condensate.

The exergy efficiency of each pressure reduction valve is the ratio of the fluid flow total exergy at the valve outlet and fluid flow total exergy at the valve inlet, as presented for PRV1 in Eq. (20). Figure 5 shows that pressure reduction valves that operate with superheated steam have a very high exergy efficiency (99.00% or higher), the highest exergy efficiency referring to PRV1 (99.75%) that operates with steam of the highest pressure and temperature (compared with other valves that operate with superheated steam).

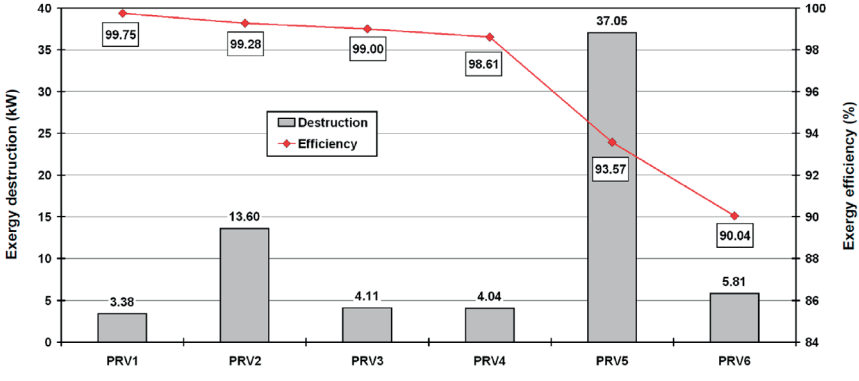

Figure 5 – Exergy destruction and exergy efficiency for all observed pressure reduction valves

Pressure reduction valves that operate with condensate have much lower exergy efficiencies on the average than valves that operate with superheated steam, Fig. 5. Considering condensate operating pressure reduction valves, the highest exergy efficiency refers to PRV4 (98.61%) whereafter it decreases to 93.57% (PRV5) and the lowest calculated exergy efficiency refers to PRV6 (90.04%).

The most important parameter defining the pressure reduction valve exergy efficiency is the operating fluid temperature, immediately followed by the operating fluid pressure. Decreases in temperature of the operating fluid passing through a valve resulted in decrease in the pressure reduction valve exergy efficiency, what makes a valid conclusion in general. In some situations, significant decrease in the operating fluid pressure can result in decrease in the valve exergy efficiency, even where the fluid temperature increases. This phenomenon can be noted comparing the operating fluid parameters for PRV2 and PRV3, Table 1.

5.2. Thermodynamic analysis of pressure reduction valves during the ambient temperature change

The ambient temperature between 278 K and 313 K can be expected in the LNG carrier steam power plant during the exploitation. Within this range it was investigated how exergy destruction and exergy efficiency of each analyzed pressure reduction valve are influenced by changes in the ambient temperature.

In observing changes in the exergy destruction of each pressure reduction valve during the ambient temperature change, it should be noted that distinction should be made between two types of analyzed valves - pressure reduction valves with exergy destruction of low-rate influence by the ambient temperature change (a change of 1 kW or lower) and valves with exergy destruction significantly influenced by the ambient temperature change (a change of more than 1 kW) within the observed ambient temperature range.

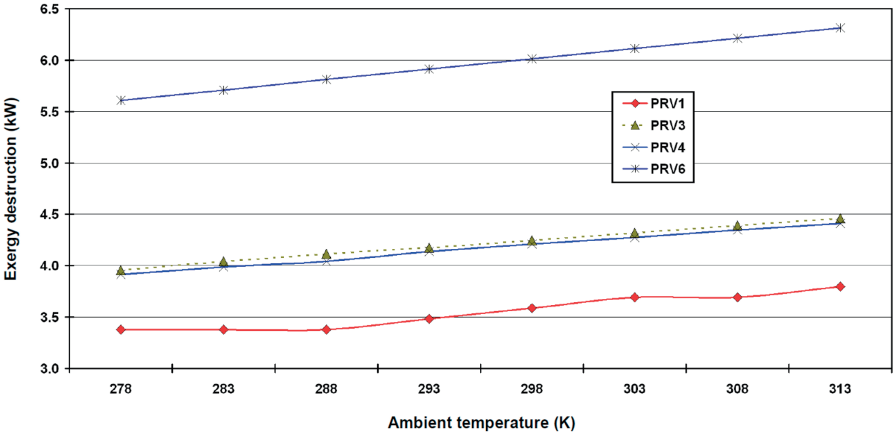

Figure 6 – Change in the ambient temperature - analyzed pressure reduction valves with small change in exergy destruction

Pressure reduction valves with exergy destruction of low-rate influence by the ambient temperature change are PRV1, 3, 4 and 6, Figure 6. The PRV1 exergy destruction is the least influenced by the ambient temperature change (from 3.38 kW at 278 K to 3.80 kW at 313 K) when all the observed pressure reduction valves are taken into account. In Figure 6, pressure reduction valve with exergy destruction most influenced by the ambient temperature change is PRV6 (from 5.61 kW at 278 K to 6.32 kW at 313 K).

Of all analyzed pressure reduction valves, PRV2 and PRV5 are the only two valves with the exergy destruction change higher than 1 kW within the observed ambient temperature range, Figure 7. Between ambient temperatures of 278 K and 313 K, the PRV2exergy destruction increases from 13.43 kW to 14.79 kW, while in the same ambient temperature range the PRV5 exergy destruction increases from 35.76 kW to 40.27 kW.

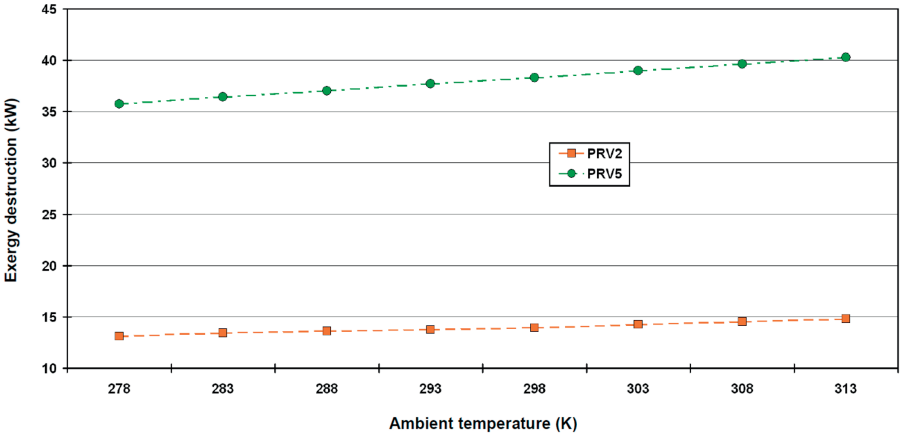

Figure 7 – Change in the ambient temperature - analyzed pressure reduction valves with the notable change in exergy destruction

It can be concluded from Figure 6 and Figure 7 that an increase in the ambient temperature results in a continuous increase in the exergy destruction of all analyzed pressure reduction valves. Another conclusion obtained from the ambient temperature variation is that changes in the ambient temperature results in a notable change in the exergy destruction of pressure reduction valves with exergy highest rate destruction at the base ambient state - as can be seen from Figure 5 and Figure 7 that the respective valves are PRV2 and PRV5.

During the ambient temperature change within the observed range, the analyzed pressure reduction valves should also be divided in two types where exergy efficiency is concerned - pressure reduction valves with exergy efficiency of low-rate influence by the ambient temperature change (a change of 1% or lower) and valves with exergy efficiency is high influence by the ambient temperature change (a change of more than 1%).

Pressure reduction valves with the exergy efficiency low-rate influenced by the ambient temperature change are PRV1, 2, 3 and 4, Figure 8. As for exergy destruction, of all observed pressure reduction valves PRV1 exergy efficiency is also the lowest influenced by the ambient temperature change (from 99.76% at 278 K to 99.67% at 313 K). From Figure 8, pressure reduction valve with the exergy efficiency most influenced by the ambient temperature change is PRV4 (from 98.77% at 278 K to 98.07% at 313 K).

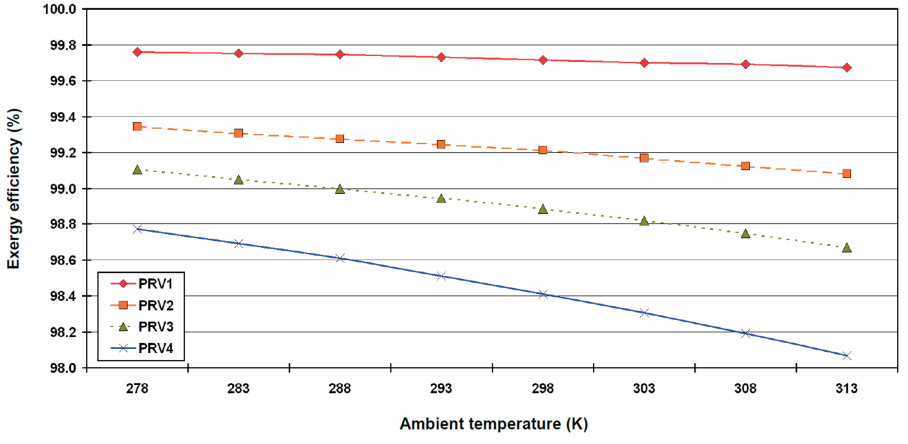

Figure 8 – Change in the ambient temperature - analyzed pressure reduction valves with small change in exergy efficiency

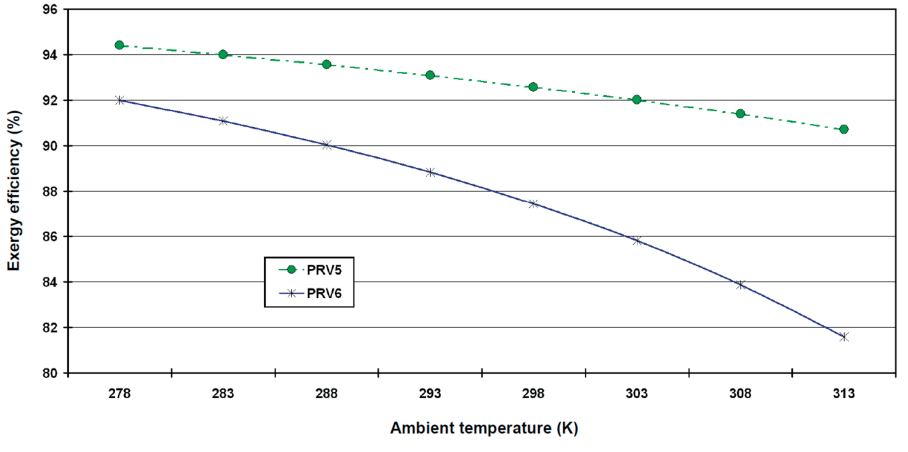

Figure 9 – Change in the ambient temperature - analyzed pressure reduction valves with notable change in exergy efficiency

PRV5 and PRV6 are the only two valves with the exergy efficiency change higher than 1% within the observed ambient temperature range, Figure 9. Between the ambient temperatures of 278 K and 313 K, exergy efficiency of PRV5 decreases from 94.41% to 90.73%, while in the same ambient temperature range exergy efficiency of PRV6 decreases from 91.99% to 81.58%, Figure 9.

It can be concluded from Figure 8 and Figure 9 that an increase in the ambient temperature results in continuous decrease in exergy efficiency of all analyzed pressure reduction valves.

Exergy efficiency of pressure reduction valves PRV5 and PRV6 is the most influenced by the ambient temperature change. Those two pressure reduction valves have the lowest exergy efficiency at the base ambient state (when all observed pressure reduction valves are taken into account), Figure 5.

6. Conclusions

This paper presents a thermodynamic analysis of pressure reduction valves from the marine steam power plant with steam re-heating that operates on conventional LNG carriers. Power plant consists of six pressure reduction valves - three of them reduce the pressure of superheated steam while the other three reduce the pressure of water/condensate. Each valve is presented its total energy/exergy flow streams, decreases in the pressure (and simultaneous temperature) of the operating fluid that passes through the valve as well as the exergy efficiency and exergy destruction. The exergy analysis enables variation of the ambient temperature and the investigation also involves changes in the exergy destruction and exergy efficiency of each observed valve during the ambient temperature change. Here are the most important conclusions of the analysis performed:

- Pressure reduction valves that operate with water/condensate cause much higher decrease in the operating fluid pressure and temperature in comparison with valves that operate with superheated steam.
- The average value of the total fluid flow energy/exergy is notably higher for pressure reduction valves that operate with superheated steam in comparison with valves that operate with water/condensate.
- Trends of the total energy and exergy fluid flow streams through each valve are of equal values.
- Pressure reduction valves that operate with superheated steam have lower average exergy destruction and higher average exergy efficiency compared with those that operate with water/condensate.
- The most important parameter that defines the pressure reduction valve exergy efficiency is the operating fluid temperature followed by the operating fluid pressure - higher operating fluid temperature in most of the cases will result in higher valve exergy efficiency.

- An increase in the ambient temperature resulted in a continuous increase in exergy destruction and in a continuous decrease in exergy efficiency for all the observed pressure reduction valves.
- Pressure reduction valves with high exergy destruction and low exergy efficiency will be notably influenced by the ambient temperature change.

Acknowledgment

This work has been fully supported by the Croatian Science Foundation under Project IP-2018-01-3739.

Nomenclature

Abbreviations:

LNG	Liquefied Natural Gas
ORC	Organic Rankine Cycle
PRV	Pressure Reduction Valve

Latin Symbols:

$\dot{E}$	total energy/exergy of a flow (kW)
h	specific enthalpy (kJ/kg)
$\dot{m}$	mass flow rate (kg/s)
p	pressure (kPa)
P	power (kW)
$\dot{Q}$	heat transfer (kW)
s	specific entropy (kJ/kg·K)
T	temperature (K)
$\dot{X}_{heat}$	exergy transfer by heat (kW)

Greek symbols:

ε	specific exergy (kJ/kg)
η	efficiency (%)

Subscripts:

0	ambient state
D	destruction (loss)
en	energy
ex	exergy
in	inlet (input)
out	outlet (output)
TOT	total

References

1. Mrzljak, V., Medica, V., Bukovac, O.: Simulation of a two-stroke slow speed diesel engine using a quasi-dimensional model, Transactions of FAMENA Vol.40, No.2, p. 35-44, 2016. (doi:10.21278/TOF.40203)
2. Ryu, Y., Lee, Y., Nam, J.: Performance and emission characteristics of additives-enhanced heavy fuel oil in large two-stroke marine diesel engine, Fuel 182, p. 850–856, 2016. (doi:10.1016/j.fuel.2016.06.029)
3. Mrzljak, V., Medica, V., Bukovac, O.: Volume agglomeration process in quasi-dimensional direct injection diesel engine numerical model, Energy 115, p. 658-667, 2016. (doi:10.1016/j.energy.2016.09.055)
4. Mrzljak, V., Medica, V., Bukovac, O.: Quasi-dimensional diesel engine model with direct calculation of cylinder temperature and pressure, Technical Gazette 24 (3), p. 681-686, 2017. (doi:10.17559/TV-20151116115801)
5. Fernández, I. A., Gómez, M. R., Gómez, J. R., Insua, A. A. B.: Review of propulsion systems on LNG carriers, Renewable and Sustainable Energy Reviews 67, p. 1395–1411, 2017. (doi:10.1016/j.rser.2016.09.095)
6. Raj, R., Ghandehariun, S., Kumar, A., Geng, J., Linwei, M.: A techno-economic study of shipping LNG to the Asia-Pacific from Western Canada by LNG carrier, Journal of Natural Gas Science and Engineering 34, p. 979-992, 2016. (doi:10.1016/j.jngse.2016.07.024)
7. Huang, H., Lv, D., Zhu, J., Zhu, Z., Chen, Y., Pan, Y., Pan, M.: Development of a new reduced diesel/natural gas mechanism for dual-fuel engine combustion and emission prediction, Fuel 236, p. 30-42, 2019. (doi:10.1016/j.fuel.2018.08.161)
8. Yousefi, A., Guo, H., Birouk, M.: Effect of diesel injection timing on the combustion of natural gas/diesel dual-fuel engine at low-high load and low-high speed conditions, Fuel 235, p. 838-846, 2019. (doi:10.1016/j.fuel.2018.08.064)
9. Attah, E. E., Bucknall, R.: An analysis of the energy efficiency of LNG ships powering options using the EEDI, Ocean Engineering 110, part B, p. 62-74, 2015. (doi:10.1016/j.oceaneng.2015.09.040)
10. Chang, D., Rhee, T., Nam, K., Chang, K., Lee, D., Jeong, S.: A study on availability and safety of new propulsion systems for LNG carriers, Reliability Engineering and System Safety 93, p. 1877– 1885, 2008. (doi:10.1016/j.ress.2008.03.013)
11. Dorosz, P., Wojcieszak, P., Malecha, Z.: Exergetic Analysis, Optimization and Comparison of LNG Cold Exergy Recovery Systems for Transportation, Entropy 20(1), 59, 2018. (doi:10.3390/e20010059)
12. Senary, K., Tawfik, A., Hegazy, E., Ali, A.: Development of a waste heat recovery system onboard LNG carrier to meet IMO regulations, Alexandria Engineering Journal 55, Issue 3, p. 1951–1960, 2016. (doi:10.1016/j.aej.2016.07.027)
13. Soffiato, M., Frangopoulos, C. A., Manente, G., Rech, S., Lazzaretto, A.: Design optimization of ORC systems for waste heat recovery on board a LNG carrier, Energy Conversion and Management 92, p. 523–534, 2015. (doi:10.1016/j.enconman.2014.12.085)
14. Zhao, F., Yang, W., Tan, W. W., Yu, W., Yang, J., Chou, S. K.: Power management of vessel propulsion system for thrust efficiency and emissions mitigation, Applied Energy 161, p. 124–132, 2016. (doi:10.1016/j.apenergy.2015.10.022)
15. Gašpar, G., Poljak, I., Orović, J.: Computerized planned maintenance system software models, Scientific Journal of Maritime Research 32 (1), p. 141-145, 2018. (doi:10.31217/p.32.1.14)
16. Trivyza, N. L., Rentizelas, A., Theotokatos, G.: A novel multi-objective decision support method for ship energy systems synthesis to enhance sustainability, Energy Conversion and Management 168, p. 128–149, 2018. (doi:10.1016/j.enconman.2018.04.020)

17. Koroglu, T., Sogut, O. S.: Conventional and Advanced Exergy Analyses of a Marine Steam Power Plant, Energy 163, p. 392-403, 2018. (doi:10.1016/j.energy.2018.08.119)
18. Mrzljak, V., Poljak, I., Medica-Viola, V.: Dual fuel consumption and efficiency of marine steam generators for the propulsion of LNG carrier, Applied Thermal Engineering 119, p. 331–346, 2017. (doi:10.1016/j.applthermaleng.2017.03.078)
19. Orović, J., Mrzljak, V., Poljak, I.: Efficiency and Losses Analysis of Steam Air Heater from Marine Steam Propulsion Plant, Energies 2018, 11 (11), 3019, (doi:10.3390/en11113019)
20. Mrzljak, V., Prpić-Oršić, J., Senčić, T.: Change in Steam Generators Main and Auxiliary Energy Flow Streams During the Load Increase of LNG Carrier Steam Propulsion System, Scientific Journal of Maritime Research 32 (1), p. 121-131, 2018. (doi:10.31217/p.32.1.15)
21. Hajebzadeh, H., Ansari, A. N. M., Niazi, S.: Mathematical modeling and validation of a 320 MW tangentially fired boiler: A case study, Applied Thermal Engineering 146, p. 232–242, 2019. (doi:10.1016/j.applthermaleng.2018.09.102)
22. Wang, C., Zhu, Y.: Entransy analysis on boiler air pre-heater with multi-stage LHS unit, Applied Thermal Engineering 130, p. 1139–1146, 2018. (doi:10.1016/j.applthermaleng.2017.11.085)
23. Mrzljak, V., Poljak, I., Prpić-Oršić, J.: Exergy analysis of the main propulsion steam turbine from marine propulsion plant, Shipbuilding: Theory and Practice of Naval Architecture, Marine Engineering and Ocean Engineering Vol. 70., No. 1, p. 59-77, 2019. (doi:10.21278/brod70105)
24. Taylor, D. A.: Introduction to Marine Engineering, Elsevier Butterworth-Heinemann, 1998.
25. Mrzljak, V., Senčić, T., Žarković, B.: Turbogenerator Steam Turbine Variation in Developed Power: Analysis of Exergy Efficiency and Exergy Destruction Change, Modelling and Simulation in Engineering 2018. (doi:10.1155/2018/2945325)
26. Mrzljak, V.: Low power steam turbine energy efficiency and losses during the developed power variation, Technical Journal 12 (3), p. 174-180, 2018. (doi:10.31803/tg-20180201002943)
27. Medica-Viola, V., Pavković, B., Mrzljak, V.: Numerical model for on-condition monitoring of condenser in coal-fired power plants, International Journal of Heat and Mass Transfer 117, p. 912–923, 2018. (doi:10.1016/j.ijheatmasstransfer.2017.10.047)
28. Laskowski, R.: Relations for steam power plant condenser performance in off-design conditions in the function of inlet parameters and those relevant in reference conditions, Applied Thermal Engineering 103, p. 528–536, 2016. (doi:10.1016/j.applthermaleng.2016.04.127)
29. Poljak, I., Orović, J., Mrzljak, V.: Energy and Exergy Analysis of the Condensate Pump During Internal Leakage from the Marine Steam Propulsion System, Scientific Journal of Maritime Research 32 (2), p. 268-280, 2018. (doi:10.31217/p.32.2.12)
30. Mrzljak, V., Poljak, I., Medica-Viola, V.: Energy and Exergy Efficiency Analysis of Sealing Steam Condenser in Propulsion System of LNG Carrier, International Journal of Maritime Science & Technology "Our Sea" 64 (1), p. 20-25, 2017. (doi:10.17818/NM/2017/1.4)
31. Mrzljak, V., Poljak, I., Medica-Viola, V.: Efficiency and losses analysis of low-pressure feed water heater in steam propulsion system during ship manoeuvring period, Scientific Journal of Maritime Research 30, p. 133-140, 2016. (doi:10.31217/p.30.2.6)
32. Moran M., Shapiro H., Boettner, D. D., Bailey, M. B.: Fundamentals of engineering thermodynamics, Seventh edition, John Wiley and Sons, Inc., 2011.
33. Burin, E. K., Vogel, T., Multhaupt, S., Thelen, A., Oeljeklaus, G., Gorner, K., Bazzo, E.: Thermodynamic and economic evaluation of a solar aided sugarcane bagasse cogeneration power plant, Energy 117, Part 2, p. 416-428, 2016. (doi:10.1016/j.energy.2016.06.071)
34. Mrzljak, V., Poljak, I., Medica-Viola, V.: Thermodynamic analysis of high-pressure fed water heater in steam propulsion system during exploitation, Shipbuilding: Theory and Practice of Naval Architecture, Marine Engineering and Ocean Engineering 68 (2), p. 45-61, 2017. (doi:10.21278/brod68204)

35. Kowalczyk, T., Ziółkowski, P., Badur, J.: Exergy Losses in the Szewalski Binary Vapor Cycle, Entropy 17, p. 7242-7265, 2015. (doi:10.3390/e17107242)
36. Noroozian, A., Mohammadi, A., Bidi, M., Ahmadi, M. H.: Energy, exergy and economic analyses of a novel system to recover waste heat and water in steam power plants, Energy Conversion and Management 144, p. 351–360, 2017. (doi:10.1016/j.enconman.2017.04.067)
37. Bruk, E., Marinčić, E., Orović, J.: The optimization of the steam plant by means of an engine room simulator, Pomorstvo 24(1), p. 41–52, 2010. (https://hrcak.srce.hr/54927)
38. Mrzljak, V., Poljak, I., Žarković, B.: Exergy Analysis of Steam Pressure Reduction Valve in Marine Propulsion Plant on Conventional LNG Carrier, International Journal of Maritime Science & Technology "Our Sea" 65(1), p. 24-31, 2018. (doi:10.17818/NM/2018/1.4)
39. Tan, H., Shan, S., Nie, Y., Zhao, Q.: A new boil-off gas re-liquefaction system for LNG carriers based on dual mixed refrigerant cycle, Cryogenics 92, p. 84–92, 2018. (doi:10.1016/j.cryogenics.2018.04.009)
40. Taheri, M. H., Mosaffa, A. H., Garousi Farshi, L.: Energy, exergy and economic assessments of a novel integrated biomass based multigeneration energy system with hydrogen production and LNG regasification cycle, Energy 125, p. 162-177, 2017. (doi:10.1016/j.energy.2017.02.124)
41. Kumar, S., Kumar, D., Memon, R. A., Wassan, M. A., Ali, M. S.: Energy and Exergy Analysis of a Coal Fired Power Plant, Mehran University Research Journal of Engineering & Technology 37 (4), p. 611-624, 2018. (doi:10.22581/muet1982.1804.13)
42. Cengel Y., Boles M.: Thermodynamics an engineering approach, Eighth edition, McGraw-Hill Education, 2015.
43. Ahmadi, G., Toghraie, D., Akbari, O. A.: Solar parallel feed water heating repowering of a steam power plant: A case study in Iran, Renewable and Sustainable Energy Reviews 77, p. 474–485, 2017. (doi:10.1016/j.rser.2017.04.019)
44. Ahmadi, G. R., Toghraie, D.: Energy and exergy analysis of Montazeri Steam Power Plant in Iran, Renewable and Sustainable Energy Reviews 56, p. 454–463, 2016. (doi:10.1016/j.rser.2015.11.074)
45. Kanoğlu, M., Çengel, Y.A., Dincer, I.: Efficiency Evaluation of Energy Systems, Springer Briefs in Energy, Springer, 2012. (doi:10.1007/978-1-4614-2242-6)
46. Adibhatla, S., Kaushik, S. C.: Energy, exergy, economic and environmental (4E) analyses of a conceptual solar aided coal fired 500 MWe thermal power plant with thermal energy storage option, Sustainable Energy Technologies and Assessments 21, p. 89–99, 2017. (doi:10.1016/j.seta.2017.05.002)
47. Bühler, F., Van Nguyen, T., Kjær Jensen, J., Müller Holm, F., Elmegaard, B.: Energy, exergy and advanced exergy analysis of a milk processing factory, Energy 162, p. 576-592, 2018. (doi:10.1016/j.energy.2018.08.029)
48. Adibhatla, S., Kaushik, S. C.: Energy and exergy analysis of a super critical thermal power plant at various load conditions under constant and pure sliding pressure operation, Applied Thermal Engineering 73, p. 49-63, 2014. (doi:10.1016/j.applthermaleng.2014.07.030)
49. Adibhatla, S., Kaushik, S. C.: Energy, exergy and economic (3E) analysis of integrated solar direct steam generation combined cycle power plant, Sustainable Energy Technologies and Assessments 20, p. 88–97, 2017. (doi:10.1016/j.seta.2017.01.002)
50. Ameri, M., Mokhtari, H., Mostafavi Sani, M.: 4E analyses and multi-objective optimization of different fuels application for a large combined cycle power plant, Energy 156, p. 371-386, 2018. (doi:10.1016/j.energy.2018.05.039)
51. Koroglu, T., Sogut, O. S.: Advanced exergy analysis of an organic Rankine cycle waste heat recovery system of a marine power plant, Journal of Thermal Engineering 3 (2), p. 1136-1148, 2017. (doi:10.18186/thermal.298614)

52. Hafdhi, F., Khir, T., Ben Yahyia, A., Ben Brahim, A.: Energetic and exergetic analysis of a steam turbine power plant in an existing phosphoric acid factory, Energy Conversion and Management 106, p. 1230–1241, 2015. (doi:10.1016/j.enconman.2015.10.044)
53. Mrzljak, V., Poljak, I., Mrakovčić, T.: Energy and exergy analysis of the turbo-generators and steam turbine for the main feed water pump drive on LNG carrier, Energy Conversion and Management 140, p. 307–323, 2017. (doi:10.1016/j.enconman.2017.03.007)
54. Uysal, C., Kurt, H., Kwak H.-Y.: Exergetic and thermoeconomic analyses of a coal-fired power plant, International Journal of Thermal Sciences 117, p. 106-120, 2017. (doi:10.1016/j.ijthermalsci.2017.03.010)
55. Zhao, Z., Su, S., Si, N., Hu, S., Wang, Y., Xu, J., Jiang, L., Chen, G., Xiang, J.: Exergy analysis of the turbine system in a 1000 MW double reheat ultra-supercritical power plant, Energy 119, p. 540-548, 2017. (doi:10.1016/j.energy.2016.12.072)
56. Naserbegi, A., Aghaie, M., Minuchehr, A., Alahyarizadeh, Gh.: A novel exergy optimization of Bushehr nuclear power plant by gravitational search algorithm (GSA), Energy 148, p. 373-385, 2018. (doi:10.1016/j.energy.2018.01.119)
57. Cangioli, F., Chatterton, S., Pennacchi, P., Nettis, L., Ciuchicchi, L.: Thermo-elasto bulk-flow model for labyrinth seals in steam turbines, Tribology International 119, p. 359-371, 2018. (doi:10.1016/j.triboint.2017.11.016)
58. Sutton, I.: Plant Design and Operations, Elsevier Inc., 2015.
59. Kostyuk, A., Frolov, V.: Steam and gas turbines, Mir Publishers, Moscow, 1988.
60. Lemmon, E.W., Huber, M.L., McLinden, M.O.: NIST reference fluid thermodynamic and transport properties-REFPROP, version 9.0, User's guide, Colorado, 2010.